JOURNAL OF MATERIALS SCIENCE 26 (1991) 2189–2194

Stack cracking by hydrogen embrittlement in a welded pipeline steel

M. Y. B. ZAKARIA
Standard and Industrial Research Institute of Malaysia, PO Box 35, 40700 Shah Alam, Selangor Darul Ehsan, Malaysia

T. J. DAVIES
Manchester Materials Science Centre, Grosvenor Street, Manchester M1 7HS, UK

Arrays of cracks, parallel to the original plate rolling direction, were produced in a X65 microalloyed steel by hydrogen embrittlement of pipeline sections containing a weldment. A region of the heat-affected zone of the weldment was shown to have a lower yield strength ("soft" zone) than the surrounding material and cracking was concentrated in this through-thickness zone to produce the effect known as stack cracking. *In situ* cathodic hydrogen charging of tensile specimens under load led to failure by linking the rolling-plane cracks with transverse cleavage cracks, which were often initiated at inclusions. All cracking was predominantly by cleavage and failure occurred in tension in short times by hydrogen embrittlement when the applied tensile stress was above about half the uncharged yield stress. The influence of microstructure, hydrogen pressure and tensile loading conditions on the location of stack cracks and the mode of fracture is discussed.

1. Introduction

The rupture or leakage of various pipelines transporting sour oil or gas (containing unspecified amounts of H_2S) have been ascribed to hydrogen cracking [1]. More recently, a mode of hydrogen cracking called stack cracking has been identified. Stack cracks are arrays of parallel cracks in parallel-to-plate thickness orientation and usually linked by finer through-thickness cracks; these have frequently been found in fractured welded steel pipelines transporting sour oil or gas [1–10]. This kind of cracking has been associated with hydrogen-induced cracking in low-alloy high-strength steels which are otherwise known to be resistant to hydrogen-induced cracking or stress corrosion cracking in normal service. Specifications of pipeline steels for sour services have subsequently been modified to improve the resistance to this type of cracking and a particular requirement is that the sulphur content should be as low as possible; lower than 0.02% has been suggested, with a reduced manganese and carbon content and effective inclusion shape control by calcium or REM treatment [7]. However, for higher strength steels of grade X52 to X70, even with this superlow sulphur content and inclusion shape control treatment, stack cracks still occur in more severe sour environments.

The work reported in this paper was part of an investigation to elucidate the formation of stack cracks, their relation to state of stress and metallurgical features such as microstructure and inclusion content of the steel to determine possible nucleation sites for these cracks, in addition to the more specific problem of elucidating the mechanism of stack cracking in a spirally welded linepipe steel. The structural characteristics of the cracks and the subsequent fractures have also been studied in order to try to model their occurrence and fracture [11].

The steel studied was a grade X65 microalloyed steel containing niobium (Nb) and had the following chemical composition (wt %): C 0.09; Si 0.38; Mn 0.82; Cu 0.26; Ni 0.195; S 0.001; P 0.01; Nb 0.04; Al 0.04; Cr 0.025; V 0.003; Mo 0.009; Ti 0.004; O 0.002; N 0.005; Ca 0.001. The steel had been silicon and aluminium deoxidized and calcium treated for inclusion control.

The pipe was spirally welded from a coil by submerged metal arc welding. The welding sequence was that the inner (bore) side was welded first and followed immediately by the outer side.

The tensile strength of the steel (containing a weldment in mid-section) was 46.7 kgf mm^{-2}, the lower yield strength was 39.7 kgf mm^{-2} and the reduction of area was 70%.

2. Experimental procedure

Cathodic charging experiments were carried out with either load in simple tension applied constantly during charging or without applied load. Fig. 1 shows the charging rig used in the experiment. The specimens were either flat rectangular or flat tensile shaped sectioned transverse to the rolling direction of the plate and across the weld, Fig. 2. Most of the specimens contained a weldment in the mid-section except for a few specimens which consisted entirely of parent

0022–2461/91 $03.00 + .12

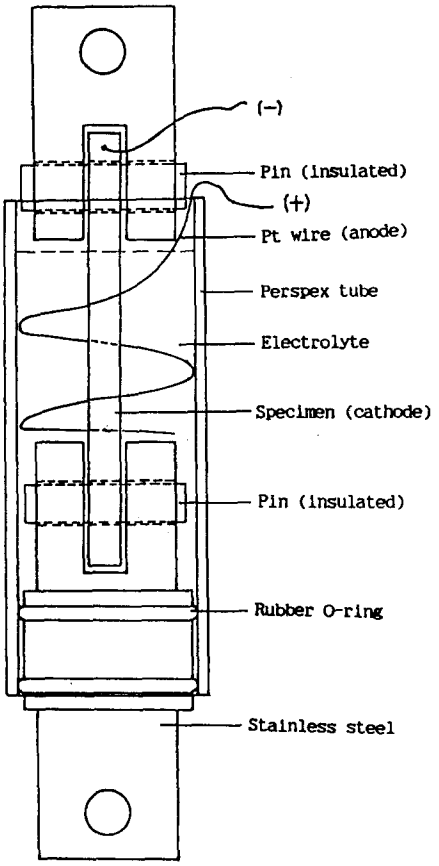

Figure 1 The charging cell.

metal. The electrolyte was 1 M H_2SO_4 + 0.4 g l^{-1} A_sO_3 and the charging current density was 10 A m^{-2}.

Flat rectangular specimens were hydrogen charged for predetermined periods under low stresses, i.e. 0.1σ_y or 0.2σ_y (σ_y = uncharged yield strength) or without applied stress. Generally, the tensile specimens were charged under relatively high stresses (0.5σ_y or 0.9σ_y) until fracture. The specimens were then sectioned for metallurgical examination by optical, SEM and/or TEM.

A number of additional specimens were modified to include geometric and structural variations, i.e. Luder's bands were introduced into some flat rectangular specimens, while notches and pressed (deformed) zones were formed in some of the flat tensile specimens prior to charging. The deformed (pressed) zone was introduced by compressing specimens between two identical hardened round rods (diameter about 9 mm). Specimens were aligned such that the width direction was parallel to the loading direction. The purpose of introducing this prior deformation was to study the effect of stress concentrations and plastic deformation on the occurrence and characteristics of the stack cracking and subsequent fracture (the pressed zone was selected to present the type of damage that could be introduced by handling and placement of a large section of pipe during pipe-laying).

3. Results and discussion

All the tensile shape specimens charged at high stresses (0.5 to 0.9σ_y) fractured with small reduction of area (0% to 15%) compared with the uncharged specimen (70%); this confirmed hydrogen embrittlement.

Stack cracks, Fig. 3, occurred most frequently in a region close to the weld, i.e. in the heat-affected zone (HAZ). Close examination revealed that this region was just outside the second HAZ and was actually in a third HAZ, which was revealed by selective etching [11] whereas this was not identified by single-stage etching. Fig. 4 shows the typical stack cracks in relation to the weldment and the HAZ regions in a section of a flat rectangular specimen. The microstructure of this region and the third HAZ retained some of the fibrous nature of the parent metal. Initial optical examination did not show any significant difference in microstructure between the region which was prone to stack cracking and the rest of the third HAZ. However, thin foil TEM examination showed the presence of carbide/cementite films at grain boundaries in this region, Fig. 5. This led to a closer optical examination of this region. Careful etching using two etchant solutions showed that cementite spheroidization had occurred in this region, Fig. 6.

Microhardness measurements showed that this region had a lower hardness than the parent metal and the rest of the third HAZ. Fig. 7 shows the microhardness profile of the uncharged specimen; the region with low hardness was about 2 to 3 mm from the weld edge. The tensile strength of specimens containing a "soft" region was also lower than the tensile strength of parent metal specimens.

The lower yield and tensile properties of the "soft" region are a consequence of the spheroidized microstructure. Tensile values for uncharged specimens showed that the difference between upper and lower yield stress in specimens containing a "soft" region was greater than in a parent metal specimen, Fig. 8. Such a high yield drop has been ascribed to a low initial mobile dislocation density [12]; such a state could exist in this soft region if dislocations were immobilized by interstitial carbon or nitrogen which migrated during the welding sequence.

Although stack cracks occurred in the parent metal, the cracking was less extensive and usually required

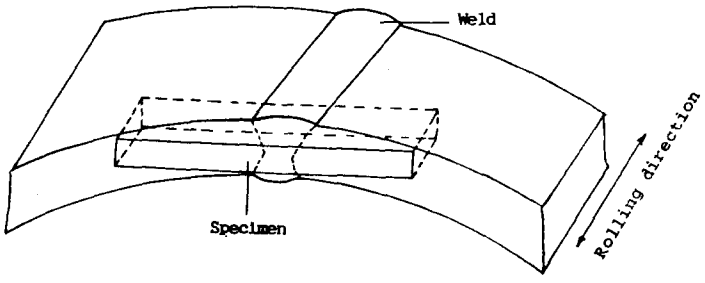

Figure 2 Sectioning of the sample to produce flat specimens.

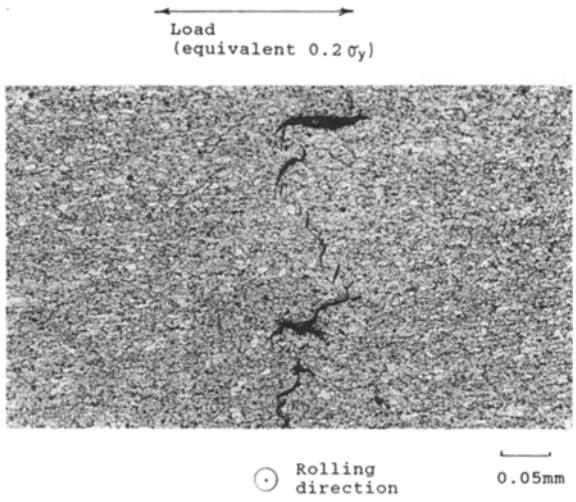

Figure 3 The characteristic array of a stack crack: note the characteristic "S" shape and the finer (vertical) cracks linking the parallel horizontal cracks.

longer hydrogen charging times. The high density of stack cracks in the soft region was probably due to the lower strength of this region requiring a lower molecular hydrogen pressure to develop cracks than in the parent metal.

The majority of cracks was found to initiate at inclusions, Fig. 9. As expected, very few of these inclusions contained sulphur, because the sulphur content of the steel was very low (0.001%). The majority of the inclusions were identified to be of the oxide, silicate or spinel type [11]. All the inclusions were globular in shape; no elongated inclusions were found although fragmentation (due to rolling) of the inclusions was detected. Most of the inclusions were of the type that were expected to produce tessellated stress [13]; hydrogen will diffuse to, and accumulate at or around, these inclusions and the subsequent pressure build-up will produce cracks.

Individual primary cracks (parallel to the plate thickness) had a characteristic "S" shape and were linked by finer transverse cracks as shown in Fig. 3. Some of these cracks were visible on the specimen surface. The cracks were found to propagate both intergranularly and transgranularly. Fig. 10 shows the outline of an individual primary (rolling plane) crack revealed by polishing and etching.

The lengths of individual cracks were not dependent on charging time, i.e. crack lengths recorded in flat rectangular specimen charged for 145, 300 and 1500 h were similar, although more cracks were found after long exposure times [11].

Stack crack formation was found to be independent of the applied stress, i.e. stack cracks were found in specimens charged without applied stress and also in specimens which had been stress relieved prior to charging. However, the applied stress level did affect the time to failure as shown by tensile specimens charged at high stresses (0.5 to 0.9σ_y). The time to failure was found to depend on the applied stress and a threshold of stress existed, above which failure occurred after a relatively short exposure time; above this threshold stress the failure time was relatively independent of the applied stress level, whereas below this threshold stress failure occurred only after long exposure times. Fig. 11 illustrates this and identifies a threshold stress of approximately 0.6σ_y.

The results of some of the additional tests demonstrated that the presence of a notch accelerated the failure process, i.e. a reduction of 20% in failure time. It was also demonstrated that prior deformation induced localization of the failure process, i.e. in those specimens which contained a pressed (deformed) zone fracture occurred at the boundary between the deformed zone and undeformed zone; it is anticipated that a residual tensile stress existed in this region. The influence of near-yield plastic deformation (Luder's bands) on susceptibility to hydrogen embrittlement was inconclusive. In the specimens containing a weldment, the Luder's band was formed in the soft region and cracking was still observed in this region, while in specimens consisting entirely of parent metal, a high incidence of cracking was observed just outside the Luder's band. It is possible that a residual tensile stress was created in the region next to the Luder's band which facilitated hydrogen diffusion and accumulation in this region.

The fracture surfaces (tensile specimens) contained cracks parallel to the plate thickness, Fig. 12. The mode of fracture consisted of cleavage rosettes with microvoids coalescence (MVC) in thin lace patterns

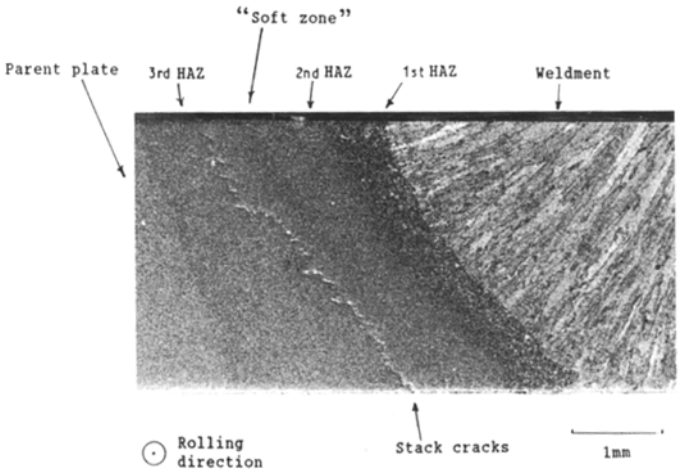

Figure 4 Stack cracks in relation to HAZs and weldment charged without load.

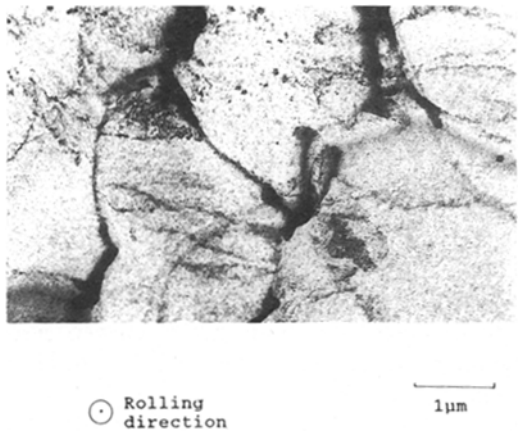

Figure 5 Cementite/carbide films at grain boundaries in the soft zone (spheroidized carbide region) identified in Figs 4 and 6.

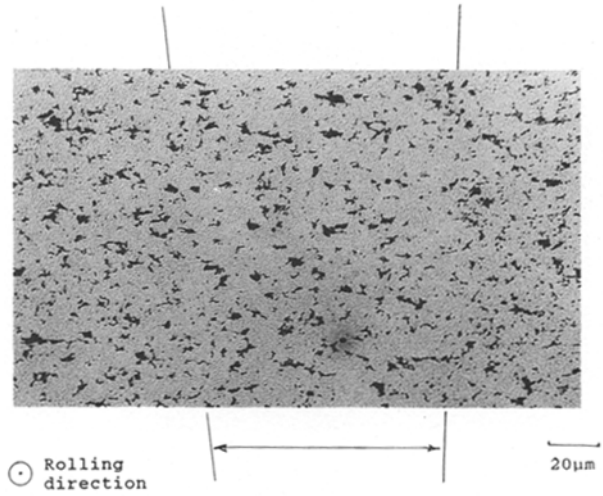

Figure 6 Region of spheroidization as revealed by selective etching with Nital, and followed by a Picral etch [11].

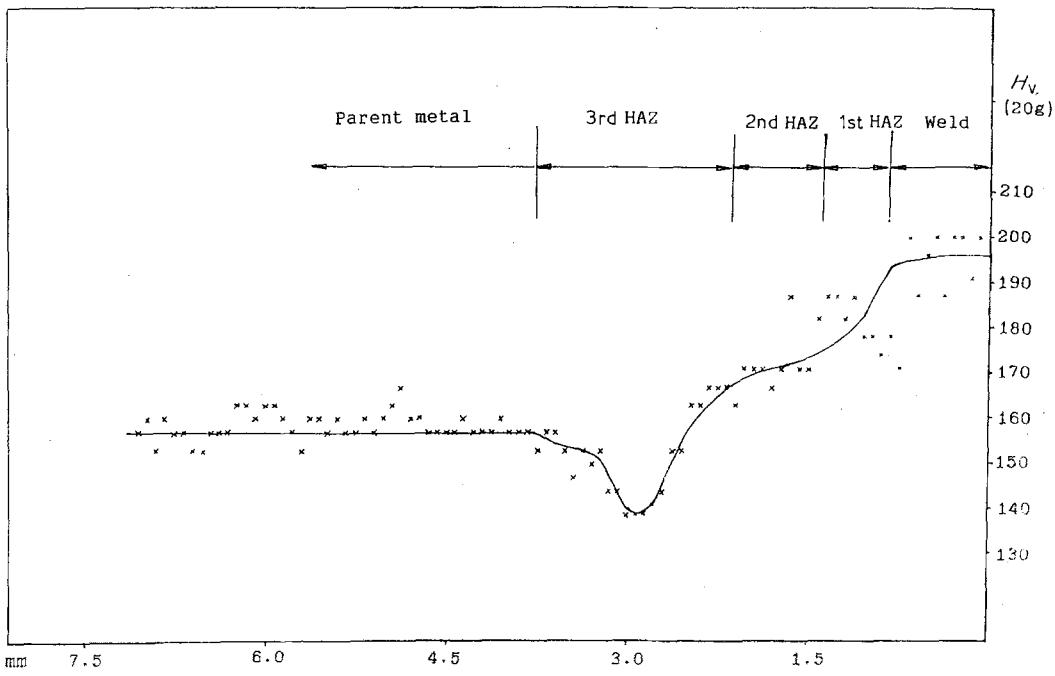

Figure 7 Microhardness profile of the sample in the as-received condition.

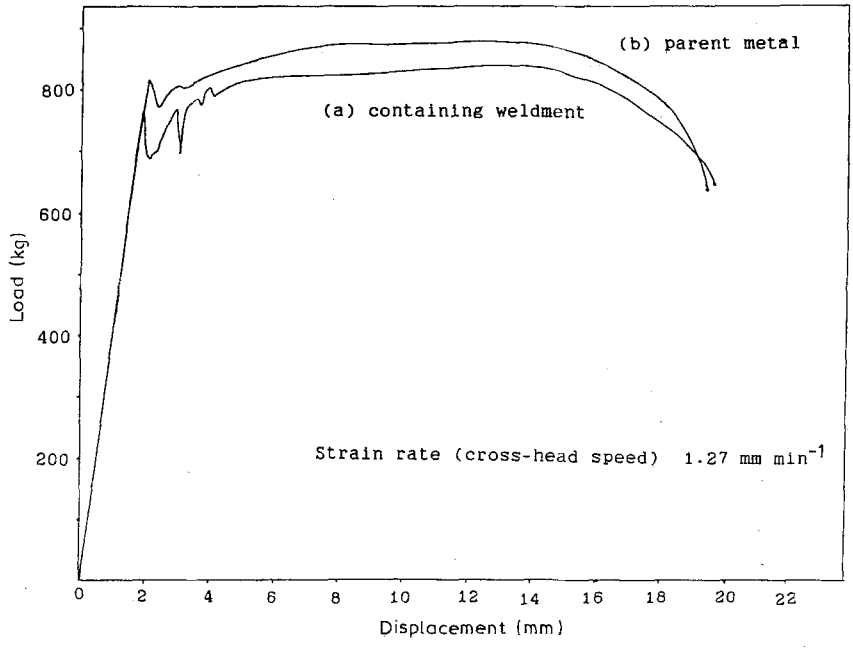

Figure 8 Load–displacement curves: (a) a specimen containing weldment, (b) a specimen consisting entirely of parent metal.

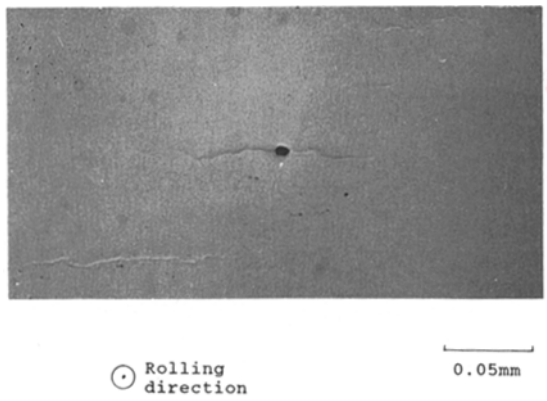

Figure 9 An incipient cleavage crack at an inclusion (charged without load).

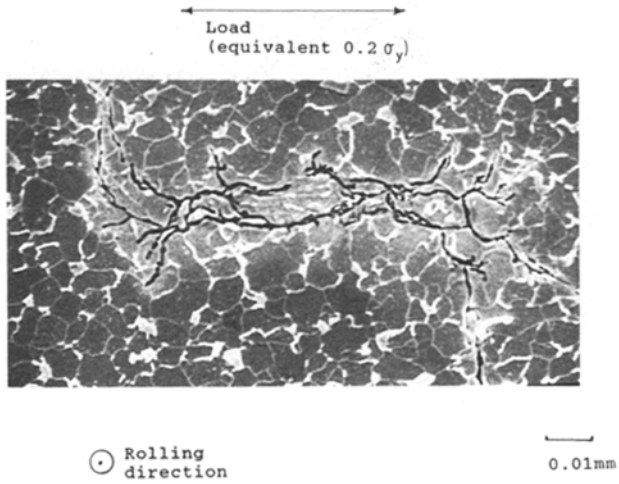

Figure 10 The outline of an individual crack showing intergranular and transgranular crack growth (the inclusions located at the centre of the cracked regions are not visible in this micrograph).

between these rosettes [11]. It is envisaged that molecular hydrogen pressure promoted the formation of the individual cleavage rosettes, including the transverse linking cracks, and final fracture occurred when the remaining ligaments between these rosettes were unable to support the applied load and failed by ductile shearing as manifested by microvoids coalescence. Thus, the final fracture was dependent on the applied stress. This was confirmed by the results of the specimens charged at $0.2\sigma_y$ where failure did not occur even after 1500 h charging, and no failure was observed in any specimens charged at low stresses or at zero stress. It was concluded that hydrogen embrittlement damage can be produced by hydrogen pressure alone and will produce severe stack cracking but will not necessarily lead to fracture in these steels.

4. Conclusions

1. Stack cracking occurred in the X65 steel under the conditions used in the experiment.

2. In general, the steel used in the experiment had a low susceptibility to hydrogen-induced cracking in normal service conditions.

3. A "soft" region was identified in the third HAZ which was very susceptible to stack cracking. Stack cracking also occurred in the parent metal but was less extensive and longer exposure times were required for cracking.

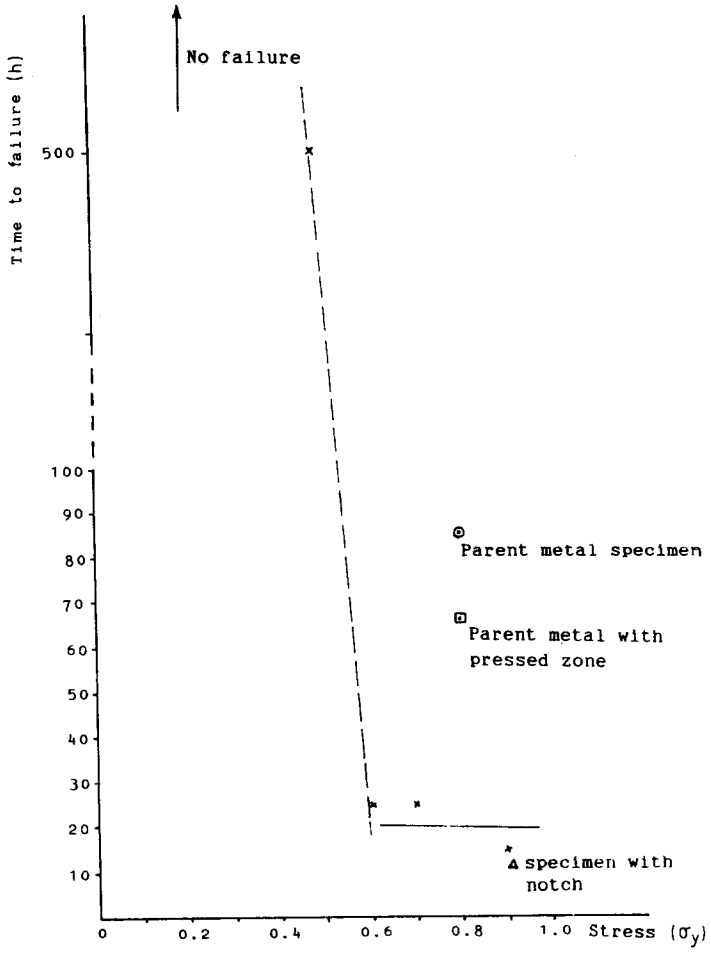

Figure 11 Failure time in relation to applied stress during hydrogen charging (specimens containing a weldment).

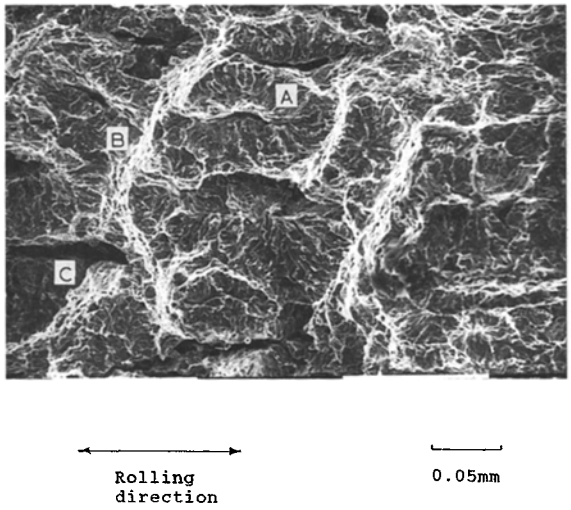

Figure 12 Typical fracture surface on a HE specimen: A, cleavage rosette normal to plane of tensile loading; B, final ligament of ductile (MVC) fracture between cleaved regions; C, rolling plane (primary) stack cracks.

4. Two types of cracks were identified: (a) primary rolling plane cracks, these had the configuration previously identified as stack cracks; (b) secondary transverse cracks which linked the primary cracks; these cracks led to fracture. Individual cracks were initiated at inclusions. No elongated inclusion was found and very few inclusions contained sulphur; oxides and silicates containing calcium were found in inclusions.

5. For the stress range used, the occurrence of stack cracks was not dependent on the stress level because cracking was also observed in specimens charged without applied stress and also in stress-relieved specimens.

6. The time to failure due to hydrogen embrittlement was found to depend on the applied stress and a stress threshold existed, above which failure occurred after a relatively short exposure time, and where failure time was independent of applied stress. The threshold stress was about $0.6\sigma_y$ for this steel.

7. Cracking was predominantly by cleavage and cracks propagated intergranularly and transgranularly. The lengths of the individual cracks were not dependent on the charging time, although more cracks were found after long exposure time.

8. The mode of fracture consisted of the formation of cleavage cracking caused by hydrogen pressure and the linking of these rosettes by microvoids coalescence when the remaining ligaments between the cleavage regions were unable to sustain the applied stress.

References

1. T. NISHIMURA, H. INAGAKI and M. TANIMURA, "Hydrogen in Metals", 2nd International Congress (1977) Paper 3E9.
2. G. J. BEIFER, *Materials Performance*, **21**(6) (1982) 19.
3. W. BRUCKHOFF, O. GEIER, K. HOFBAUER, G. SCHMITT and D. STEINMETZ, "Corrosion 85", paper 389.
4. T. TAIRA, K. TSUKADA, Y. KOBAYASHI, H. INAGAKI and T. WATANABE, *Corrosion* **37** (1981) 5.
5. GUENTER HERBSLEB, ROLF K. POEPPERLING and WILHEM SCHWENK, *ibid.* **36** (1980) 247.
6. A. BROWN and C. L. JONES, *ibid.* **40** (1984) 330.
7. T. TAIRA, Y. KOBAYASHI, K. MATSUMOTO and K. TSUKADA, *ibid.* **40** (1984) 478.
8. J. C. TURN Jr, B. E. WILDE and C. A. TROIANOS, *ibid.* **39** (1983) 364.
9. S. W. CIARALDI, *ibid.* **40** (1984) 77.
10. MAKIO IINO, *Met. Trans.* **9A** (1978) 1581.
11. M. Y. B. SAKARIA, PhD Thesis. UMIST (1989).
12. D. HULL and D. J. BACON, "Introduction to Dislocations" (Pergamon Press, 1986) Ch. 10.
13. D. BROOKSBANK and K. W. ANDREWS, *JISI* **206** (1968) 595.

Received 14 June
and accepted 22 November 1989